Climate Dynamics (2004) 23: 495–511
DOI 10.1007/s00382-004-0442-9

G. A. Meehl · C. Tebaldi · D. Nychka

Changes in frost days in simulations of twentyfirst century climate

Received: 20 March 2003 / Published online: 20 August 2004

Abstract Global coupled climate model simulations of twentieth and twentyfirst century climate are analyzed for changes in frost days (defined as nighttime minima less than freezing). The model simulations agree with the observed pattern for late twentieth century of a greater decrease of frost days in the west and southwest USA compared to the rest of the country, and almost no change in frost days in fall compared to relatively larger decreases in spring. Associated with general increases of nighttime minimum temperatures, in the future climate with increased greenhouse gases (GHGs) the number of frost days is fewer almost everywhere, but there are greatest decreases over the western parts of the continents. The numbers of frost days are most consistently related to sea level pressure, with more frost days occurring when high pressure dominates on the monthly time scale in association with clearer skies and lower nighttime minimum temperatures. Spatial patterns of relative changes of frost days are indicative of regional scale atmospheric circulation changes that affect nighttime minimum temperatures. Increases of soil moisture and clouds also contribute, but play secondary roles. The linkages among soil moisture, clouds, sea level pressure, and diurnal temperature range are quantified by a statistical multiple regression model. Coefficients for present and future climate are similar among the predictors, indicating physical processes that affect frost days in present and future climates do not appreciably change. Only the intercept changes in association with the significant warming of the mean climate state. This study highlights the fact that, though there is a general decrease in the number of frost days with global warming, the processes that affect the pattern of those changes, and thus the regional changes of frost days, are influenced by several interrelated physical processes, with changes in regional atmospheric circulation generally being most important.

G. A. Meehl (✉) · C. Tebaldi · D. Nychka
National Center for Atmospheric Research, PO Box 3000, Boulder, CO 80307, USA
E-mail: meehl@ncar.ucar.edu

1 Introduction

Changes in extreme weather and climate events can affect human societies, ecosystems and wildlife in many ways (Parmesan et al. 2000). Nighttime temperatures below 0 °C, often referred to as ''frost days'', are indicative of one of these extremes with multiple impacts. In the IPCC Third Assessment Report, it was concluded that it was ''very likely'' there would be a decrease in frost days (defined here as nighttime minimum temperatures falling below 0 °C) in a future climate. However, this was assumed to occur based on a general warming in global coupled climate models, not on any direct evidence or analyses from these models looking at changes in frost days directly. It is our aim here to analyze a global coupled model to examine directly the possible future changes in frost days in a global warming scenario. Other measures of the impacts of climate extremes, such as changes of heat index (Delworth et al. 1999), have indicated that a variety of physical processes can contribute to the actual pattern of such extremes in future climate. We will show here that this is indeed the case for changes in frost days which can have impacts on agriculture, insect hatch numbers and infestations, and ecosystems (Meehl et al. 2000; Parmesan et al. 2000; Easterling et al. 2000).

Associated with a general warming of the planet, particularly over the second half of the twentieth century, several observational studies have noted a decrease in frost days in a number of regions. Easterling (2002) documented decreases in frost days over the United States.

Bonsal et al. (2001) found similar results for Canada, and Heino et al. (1999) analyzed records for northern Europe and documented decreasing frost days in that

region during the twentieth century. Though decreases in frost days are often generally assumed to be linked to increasing nighttime temperature minima, regional patterns indicate that various processes could contribute in different ways depending on location (Easterling 2002).

Here we examine possible future regional changes in frost days in a global coupled model, and address processes that could contribute to those changes. The global coupled climate model and the experiments are described in Sect. 2. The changes in frost days from the model for twentieth and twentyfirst century are discussed in Sect. 3. Section 4 examines results for five selected regions to explore further the relationship among the processes, and in Sect. 5 we present results from a statistical model of frost day changes. In Sect. 6 we examine possible links to one definition of growing season length, and conclusions follow in Sect. 7.

2 Model and experiments

We use the fully coupled global climate model, the National Center for Atmospheric Research/Department of Energy Parallel Climate Model (PCM), which is described by Washington et al. (2000). The resolution of the atmosphere is T42, or roughly 2.8° × 2.8°, with 18 levels in the vertical. Resolution in the ocean is roughly 2/3° down to 1/2° in the equatorial tropics, with 32 levels. No flux corrections are used in the model, and a stable climate is simulated. For example, a 1000-year long control integration shows only a small cooling trend of globally averaged surface air temperatures of roughly 0.03 K per century, and the interannual climate variability related to ENSO is in reasonable agreement with observations (Meehl et al. 2001; Dai et al. 2001).

The PCM has been run for a series of four member ensemble simulations of twentieth century climate with various combinations of observed forcings, including GHGs, direct effect of sulfate aerosols, tropospheric and stratospheric ozone, solar and volcanoes (Meehl et al. 2004b; Ammann et al. 2003). Additionally, a number of future climate simulations have been performed with business-as-usual (BAU, Dai et al. 2001, similar to the average of the SRES scenarios), and a stabilization scenario (Dai et al. 2001), in addition to five different SRES scenarios (A2, B2, A1B, A1FI, B1). Here we analyze an ensemble of four BAU simulations for the end of the twentyfirst century compared to an ensemble of four twentieth century simulations with the PCM. The twentieth century simulations include observed estimates of time-evolving solar, volcano, sulfate aerosol, ozone, and greenhouse gas forcings, and are described in detail in Meehl et al. (2004b).

Surface air temperature in both model and observations is defined as the 2 m air temperature. This particular model is on the lower end of the climate sensitivity range, with an equilibrium climate sensitivity to a doubling of CO_2 of 2.1C, and a transient climate response (TCR, defined as the temperature change at the time of CO_2 doubling in a 1% per year CO_2 increase experiment) of 1.32 °C (Meehl et al. 2004a).

3 Changes in frost days

3.1 Late twentieth century over the USA

To see how well the model performs for simulating changes in frost days we have already observed, Fig. 1 compares area-averaged trends in changes in frost days for the period 1948–1999 (days per decade) from observations compiled by Easterling (2002) and from the four member ensemble mean model for twentieth century climate. Annual trends are shown in addition for the two seasons that could affect growing season length, spring (March–April–May) and fall (September–October–November). For the observations on the left in Fig. 1, the annual changes in frost days show trends for decreasing frost days that are greater over the western USA (values in excess of –2 days per decade) and southwestern USA (–1 days per decade) compared to trends approaching zero for the upper Midwest and northeastern USA. For annual values from the model in Fig. 1b, a similar pattern to the observations in Fig. 1a is seen, with largest trends for decreasing frost days in the western and southwestern USA (values greater than –2 days per decade), and trends near zero in the upper Midwest and northeastern USA. The observations are large area-averages but still reflect most of the detailed regional features seen for the model in Fig. 1b.

The biggest discrepancy between model and observations is over parts of the southeastern USA where the model shows trends for decreasing frost days and the observations show slight increases. This is thought to be a partial consequence of the two large El Nino events in the observations during this time period (1982–83 and 1997–98) where anomalously cool and wet conditions occurred over the southeastern USA and contributed to slight increases of frost days. The ensemble mean from the model averages out effects from individual El Nino events, and thus the frost day trends reflect a more general response to the forcings that occurred during the latter part of the twentieth century. To verify this relationship in the model, we stratify El Nino and La Nina years in the ensemble members and compute ensemble mean frost day differences for El Nino minus La Nina years. The results show generally negative differences west of the Rockies, and positive differences in most of the upper Midwest and parts of the southeast USA, the latter indicating more frost days during El Nino winters (not shown).

Also note the decreases of frost days over the ocean off the northeast coast of the USA (Fig. 1b). This reflects the reduction of cold air outbreaks from the North American continent that often bring sub-freezing temperatures over the ocean, and these are reduced with the warmer climate in late twentieth century.

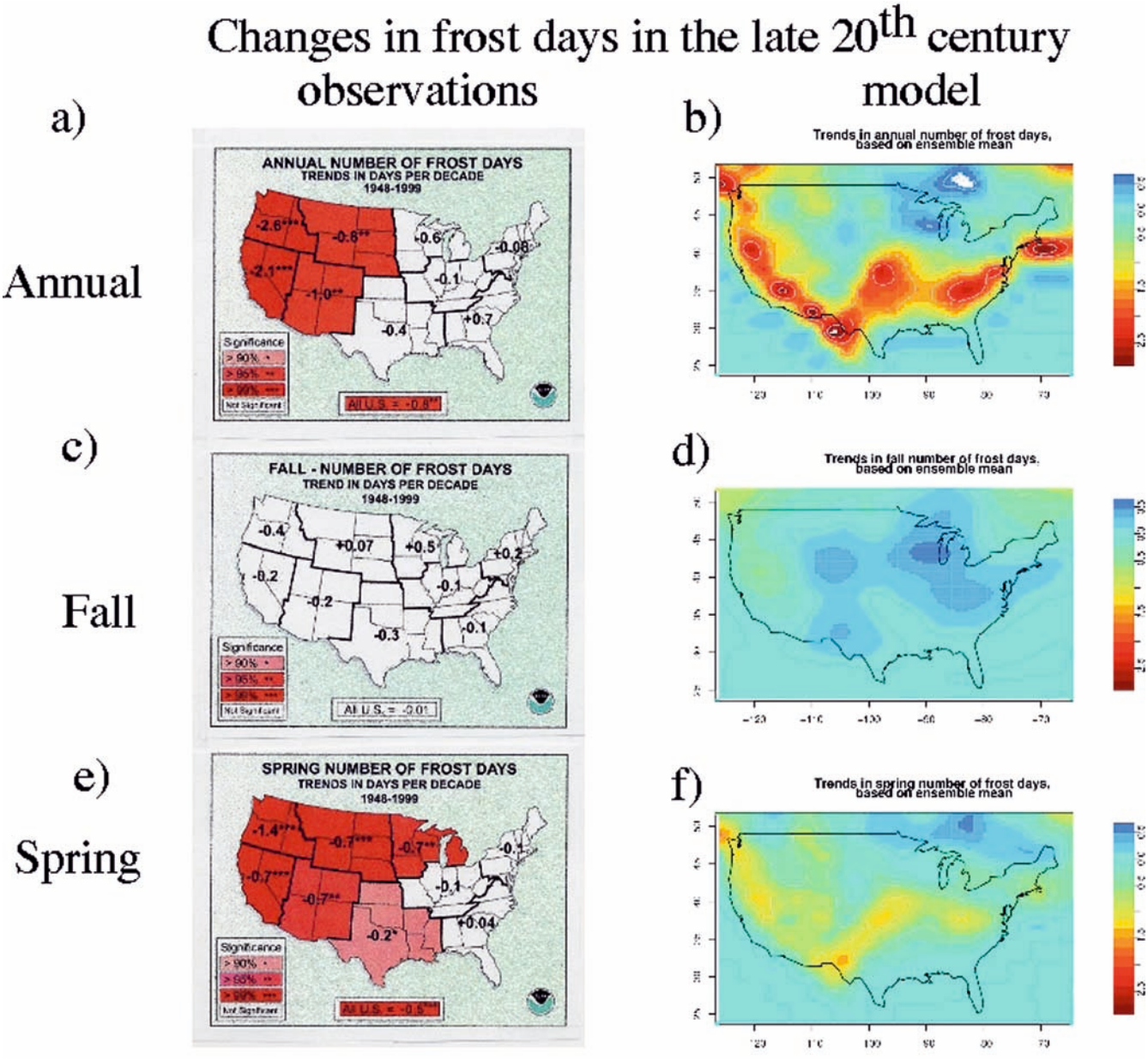

Fig. 1 Trends (days per decade) of changes in frost days for the USA for the period 1948–1999, **a** area-averaged annual observations from Easterling (2002); **b** four member ensemble annual mean from model simulation; **c** same as **a** except for fall (September–October–November) from observations; **d** same as **b** except for fall from model; **e** same as **a** except for spring (March–April–May) from observations; **f** same as **b** except for spring from model

Since changes in frost days could influence growing season length, a comparison between observations and model is shown for fall and spring. For the observations in fall (Fig. 1c), the trends for frost days are near zero over the entire USA, with slightly greater tendencies for decreases of frost days over the western USA (values of –0.2 to –0.4 days per decade). There are actually slight increases of frost days over the upper Great Plains, upper Midwest and northeastern USA. A similar pattern is seen from the model simulation of late twentieth century climate (Fig. 1d). There are small decreasing trends in frost days over parts of the western USA (less than –0.5 days per decade), with slight increases over the upper Great Plains, upper Midwest, and northeaster USA.

This is in contrast to the much greater decreases in frost days in spring in both observations and model (Fig. 1e, f). For observations, the pattern seen for annual changes in Fig. 1a is reflected in the negative trends in the spring season over much of the western USA, but with values about half of the annual ones (–0.7 to –1.4 days per decade compared to values up to –2.6 days per decade for the Pacific northwest in the annual plot in Fig. 1a; most of the rest of the changes occur in winter). Over the northeast and southeast USA there are smaller values compared to the west during spring in both model

and observations. Therefore, the basic elements of the overall pattern of greater reductions in frost days over the western USA compared to eastern USA, and greater decreases in spring compared to fall characterize both model and observations. This gives us confidence that the model is likely capable of simulating the relevant processes involved with the patterns of changing frost days for future climate.

3.2 Projections for twentyfirst century

Figure 2a shows the annual changes in frost days for the 20 year average 2080–2099 minus the twentieth century reference period 1961–1990. Associated with the general warming that occurs over this time period (Dai et al. 2001), the number of frost days decreases everywhere, with largest values of over –30 days on the west coast of

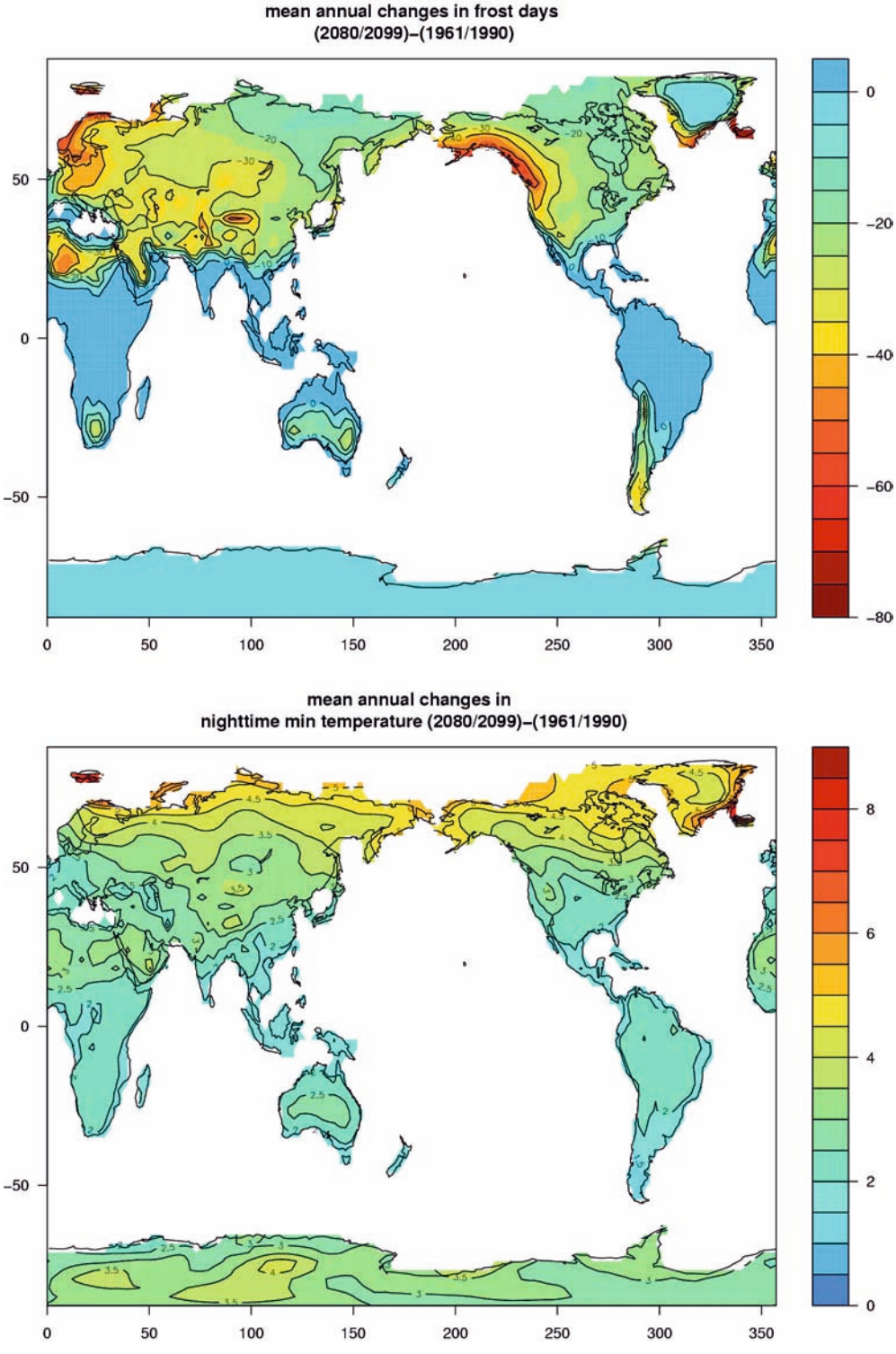

Fig. 2 **a** Differences in annual frost days, 2080–2100 minus 1961–1990 (units), and **b** differences in annual minimum temperature (°C)

North America, northern Europe and central Asia, and North Africa. In general, there is a gradient from west to east across the continents, with greater decreases in the western regions. This general pattern is similar to that documented for late twentieth century frost day changes in the previous section across the United States for model and observations. The rates of change of frost days are comparable between late twentieth and late twentyfirst century periods, consistent with the similar rates of change of radiative forcing for those two time periods (Dai et al. 2001).

As noted previously, it has been assumed that changes in frost days are linked to comparable changes in nighttime minimum temperature. These changes are shown for future climate in Fig. 2b. Unlike decreases in frost days, there are greater increases in nighttime

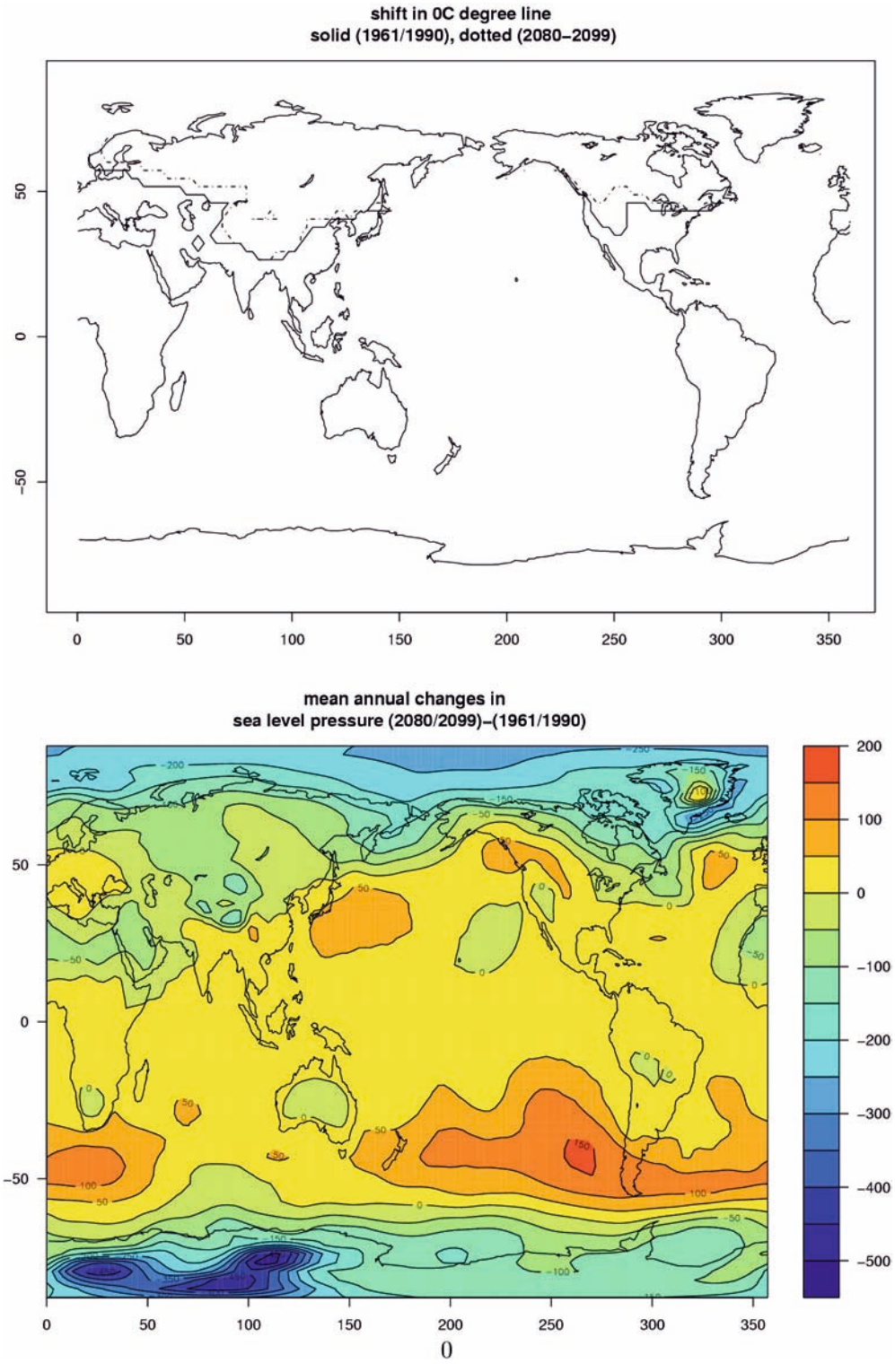

Fig. 3 **a** Position of the annual 0 °C line for present (*solid*) and future (*dashed*) climate, and **b** differences in annual sea level pressure, future minus present (Pa)

minima farther north over the northern continents (values over +3.5 °C), with lower amplitude increases over western Europe and the western USA (around +2 to +3 °C). If there was a direct relationship between changes in frost days and nighttime minima, the largest warming of nighttime minima should occur where there are greatest decreases in frost days. However, as noted and seen in Fig. 2a, b, largest increases in nighttime minima occur over the northern parts of the northern continents where there are the fewest decreases in frost days.

The relationship between nighttime minima and frost day changes is actually affected to a certain extent in the margin areas where the 0 °C line (defined as any location where the nighttime minimum reaches 0 °C during the year) changes in future climate. This is shown in Fig. 3a where the 0 °C line (for surface air temperature) is plotted for present and future climate. The changes in frost days are greatest where there is poleward movement of the 0 °C line. Therefore, even though minimum temperature increases are greatest farther poleward, the minimum temperatures still stay below 0 °C and there are fewer changes in frost days. However, the southwest-northeast gradient of frost days in Fig. 2a is not reflected in the changes in nighttime minima in Fig. 2b. Therefore, there are other processes taking place that affect changes in frost days. We examine these processes next.

Figure 3b shows ensemble mean differences in annual sea level pressure (SLP) for future climate. As seen in other models (e.g., Cubasch et al. 2001), there are general decreases of SLP of greater than 2 hPa at high latitudes in both hemispheres. However, the patterns of the changes in SLP are instructive for understanding the changes in frost days. First, for North America, there is an anomalous ridge of positive SLP differences over western Canada. This SLP anomaly pattern is associated with geostrophic southwesterly low level wind anomalies parallel to the isobars from the Pacific into Alaska, and anomalous southeasterlies from the southern USA to the Pacific northwest (not shown). This anomalous flow from relatively warmer regions produces a greater increase in temperature in western North America compared to continental areas farther east, a consequent movement of the 0 °C line (Fig. 3a), and a relatively large decrease in frost days (Fig. 2a). Meanwhile, for eastern North America, there is anomalous northwesterly geostrophic flow as indicated by the SLP differences in Fig. 3b. This advects anomalously cooler air into eastern and southeastern North America, resulting in less change of the 0 °C line and relatively fewer decreases in frost days.

Similarly for Western Europe, there is anomalous westerly flow from the Atlantic bringing more maritime air into Western and Northern Europe. This is associated with anomalously low SLP near Iceland that is the signature of the positive phase of the North Atlantic Oscillation (NAO). This change of the NAO to a more positive phase has been suggested to be a response to increasing GHGs in some model simulations (Fyfe et al. 1999; Gillett et al. 2002; Arblaster et al. in preparation 2004). This more positive phase of the NAO causes a retreat of the 0 °C line and a relatively greater decrease of frost days in Western Europe than over northeastern Asia where there is anomalous northwesterly geostrophic flow as indicated by the SLP differences in Fig. 3b. The latter is associated with less of a retreat of the 0 °C line, and relatively fewer decreases in frost days in Fig. 2a.

For South America near 30–40°S, an anomalous ridge over the southeastern Pacific is associated with blocking of the storm track that would normally bring cold air outbreaks to that region, with a consequent decrease in frost days over that part of South America.

Inspection of SLP changes in other seasons (not shown) indicates most of the annual signal shown in Fig. 3b arises from the cold season from roughly November to March. Differences in Fig. 3b greater than about 30 Pa are significant at the 5% level from a Student t test. Thus, the SLP differences over much of the midlatitude regions are significant. Cold season differences are larger (not shown), but have the same pattern, with differences in most midlatitude areas significant at the 5% level.

Therefore, it is clear from Fig. 3b that the pattern of changes in frost days is affected by increases in nighttime minima associated, in part, with anomalous low level winds in the future climate that change the source of advected air and contribute to the pattern of decreases of frost days in Fig. 2a.

4 Regional changes

The changes in SLP and associated low level winds discussed in the previous section are also likely to be associated with changes in other processes that can affect frost days. To examine these processes more closely, we select five regions for detailed analysis. The five regions are represented by single grid points in the southeast USA (34.9°N, 84.4°W), northwest USA (43.3°N, 120.9°W), eastern China (34.9°N, 115.3°E), northern Europe (51.6°N, 8.4°E), and southeast Australia (34.9°S, 143.4°E).

Figure 4 shows changes in frost days for the five regions for the reference periods (1961–1990) compared to the future climate in the BAU runs at the end of the twentyfirst century (2080–2099). The ensemble means

►

Fig. 4 **a** Frost days plotted for ensemble mean (*solid lines*) for 1961 to 1990 (*red*), and for 2080 to 2099 (*blue*), individual ensemble member time series are *dotted lines*, and range of highest and lowest value from any ensemble member per year is dashed, for southeast USA; **b** frost day anomalies for 2080 to 2099 as in **a** with linear *trend lines* added for each ensemble member; **c** same as **a** except for northwest USA; **d** same as **b** except for northwest USA; **e** same as **a** except for Northern Europe; **f** same as **b** except for Northern Europe; **g** same as **a** except for eastern China; **h** same as **b** except for eastern China.; **i** same as **a** except for southeast Australia.; **j** same as **b** except for southeast Australia

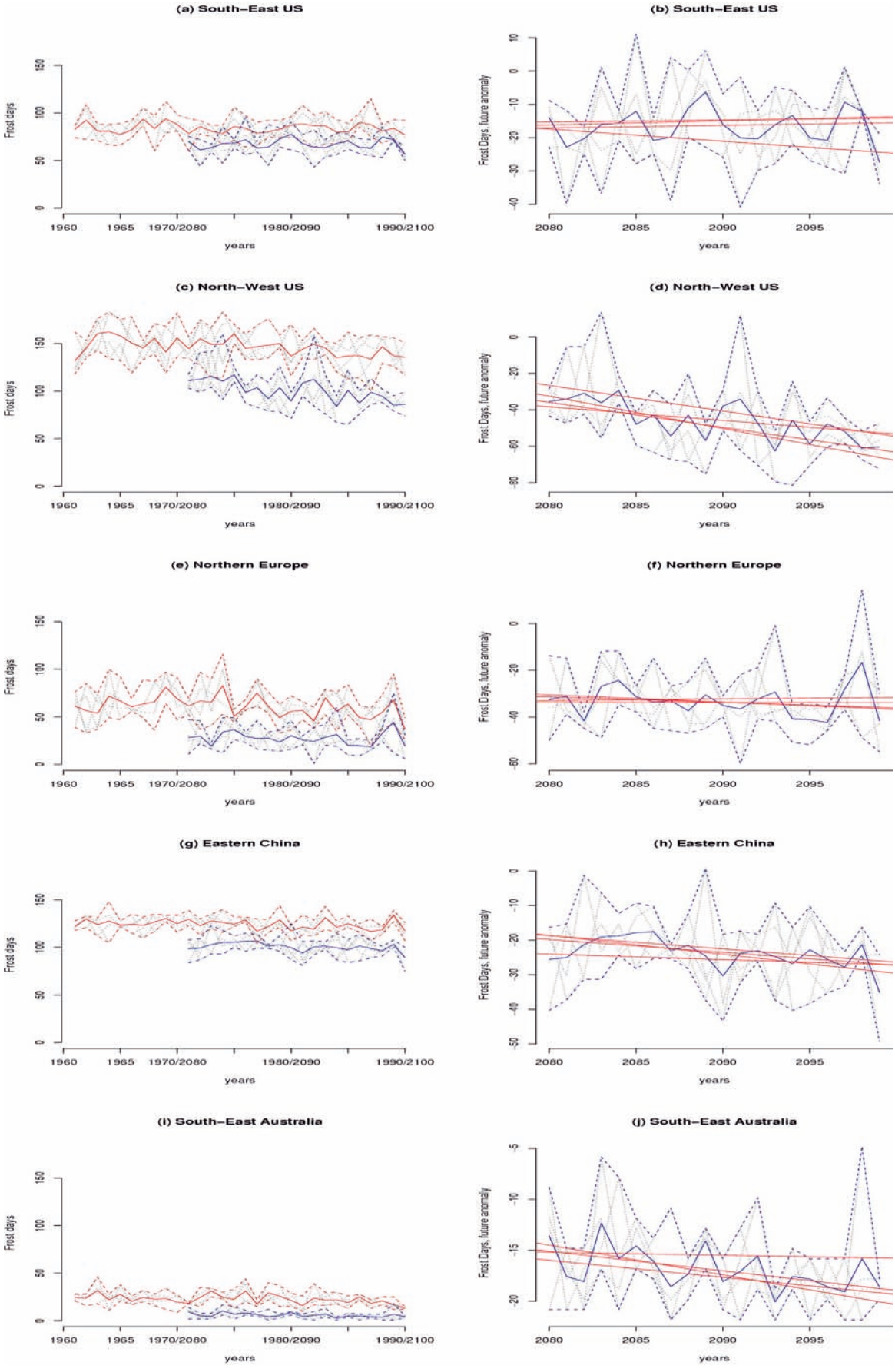
(a) South−East US
Frost days
years
1960
1965
1970/2080
1980/2090
1990/2100
(b) South−East US
Frost Days, future anomaly
2080
2085
2090
2095
(c) North−West US
(d) North−West US
(e) Northern Europe
(f) Northern Europe
(g) Eastern China
(h) Eastern China
(i) South−East Australia
(j) South−East Australia

are the solid lines, the individual ensemble members are the dots, and the spread of the ensembles (as given by the maximum and minimum values from individual ensemble members for each year) is given by the dashed lines. Also shown are the individual linear trends for future anomalies, derived from the four individual ensemble members, having subtracted from each of them the ensemble mean of the reference period (1961–1990). All five areas show significant decreases of frost days, the envelope of the anomaly time series being consistently below zero, and their trends being flat or negative for all individual time series (Fig. 4b, d, f, h, and j). Trends over the last 20 years of the twentyfirst century are largest for northwest USA compared to southeast USA reflecting the greatest decreases in frost days in the northwest USA observed in the late twentieth century (Fig. 1) and for future climate (Fig. 2a) associated in part with regional-scale changes in anomalous lower level circulation (Fig. 3b). Northern Europe also shows a relatively small trend in frost days over the late twentyfirst century period, though the absolute change from the twentieth century shows a significant decrease (Fig. 4e). There are similar results for eastern China in Fig. 4g and 4h. Southeast Australia (Fig. 4i, j) shows a significant decrease of frost days (nearing zero for the twentyfirst century) as well as a downward trend, significant in three out of four of the future ensemble members' anomalies. The ensemble means of linear trends for reference and future periods are listed in Table 2. The numbers labeled "*t*-value" are significance levels of the estimates. All five areas show negative trends for decreasing frost days in present-day (refer-

Table 1 The trend in frost days (days per year) calculated for the model ensemble means for the present reference period (1961–1990) and future (2080–2099) with *t* values. Starred *t* values indicate significance at the 5% level

		Trend	t-value
Southeast US	Present	–0.05	0.61
	Future	–0.02	0.91
Northwest US	Present	–0.51	0.00*
	Future	–1.32	0.00*
N. Europe	Present	–0.47	0.03*
	Future	–0.12	0.65
E. China	Present	–0.16	0.11
	Future	–0.37	0.02*
SE Australia	Present	–0.23	0.01*
	Future	–0.17	0.03*

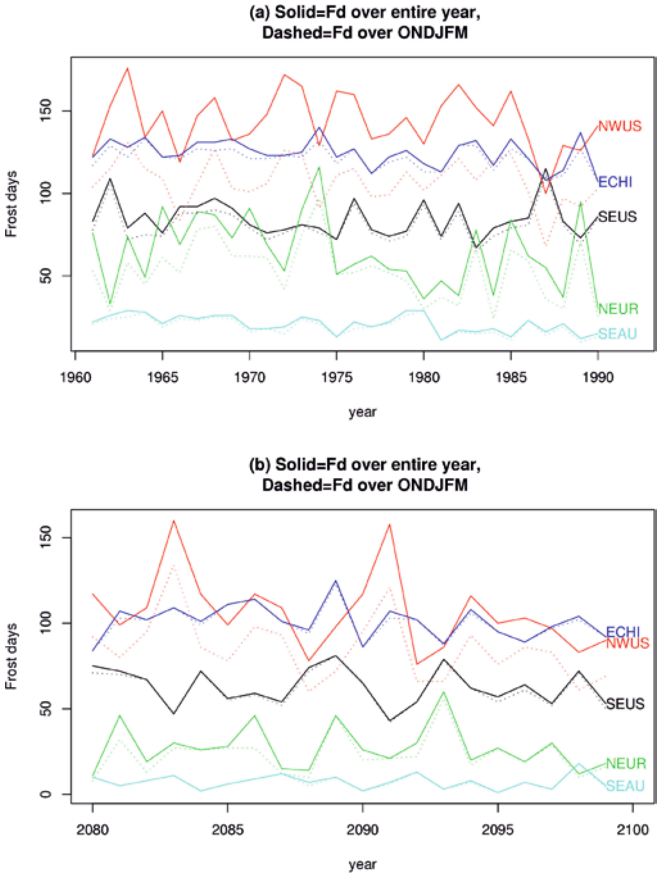

Fig. 5 **a** Time series of frost days from 1961 to 1990, *solid line* for annual values, dotted for cold season (*ONDJFM* for Northern Hemisphere, *AMJJAS* for Southern Hemisphere), for, *top* to *bottom*, northwest USA, eastern China, southeast USA, Northern Europe, and southeast Australia; **b** same as **a** except for future climate, 2080–2099

Table 2 R^2 values for the five regions for daily minimum temperature (Tmin), diurnal temperature range(ETR), total cloud(Cld), soil moisture (Soilm)and sea level pressure(SLP). Values of Southest USA and Northwest USA correspond to Fig. 6, left column, and 6, right column, respectively. Starred values indicate significance at the 1% level for the corresponding linear regression coefficient

		Tmin	ETR	Cld	Soilm	SLP
Southeast USA	Present	0.87*	0.16*	0.00	0.10*	0.18*
	Future	0.85*	0.06	0.01	0.02	0.28*
Northwest USA	Present	0.84*	0.32*	0.11*	0.40*	0.25*
	Future	0.82*	0.10*	0.00	0.15*	0.30*
N.Europe	Present	0.83*	0.02	0.16*	0.00	0.20*
	Future	0.82*	0.00	0.16*	0.01	0.30*
E.China	Present	0.75*	0.00	0.21*	0.00	0.29*
	Future	0.76*	0.40	0.24*	0.00	0.26*
SE Austraila	Present	0.74*	0.06*	0.01	0.05	0.27*
	Future	0.76*	0.04	0.34*	0.00	0.26*

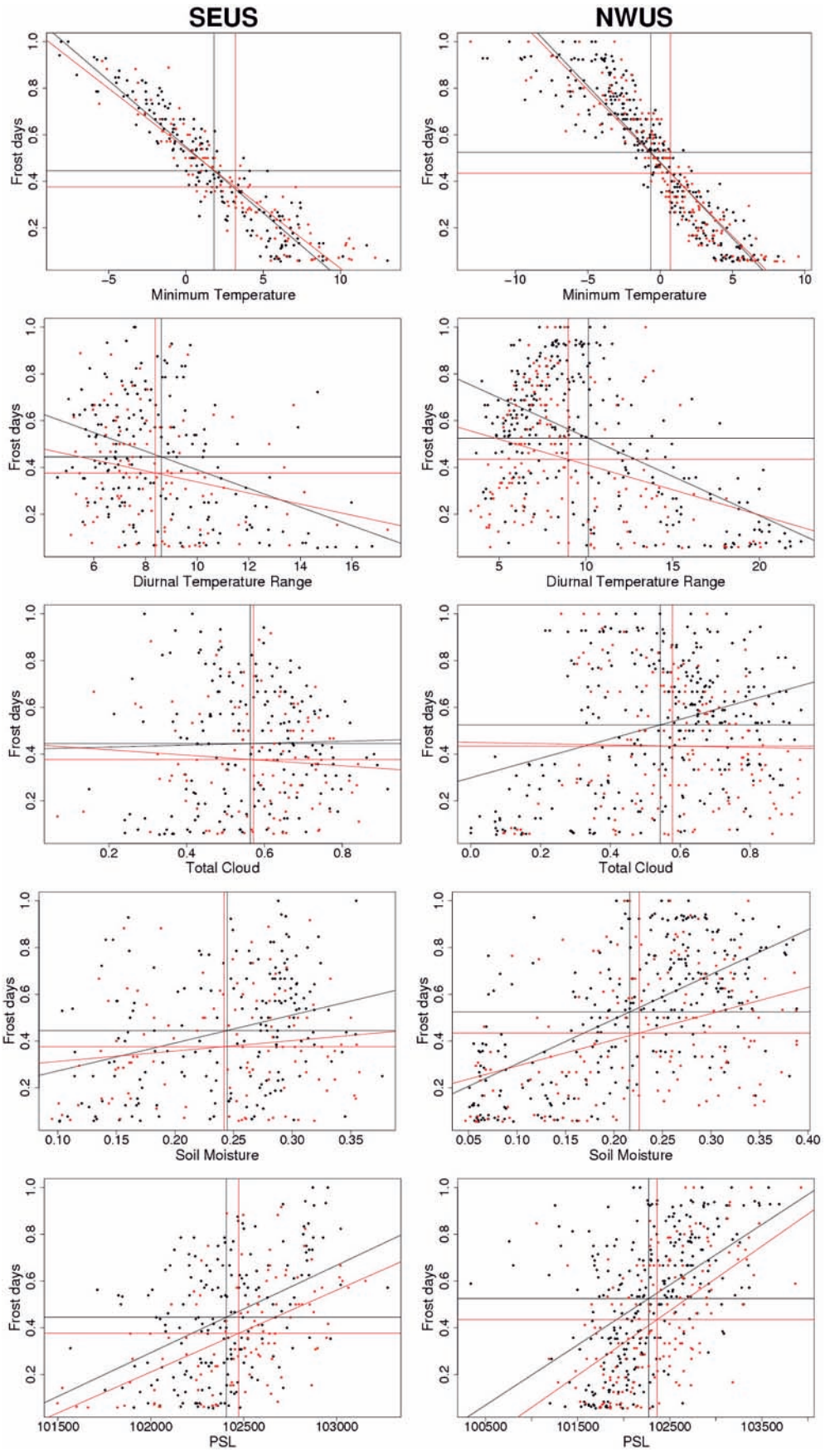

Fig. 6 *Left column*: fraction of cold season frost days plotted as a function of (*top* to *bottom*), minimum temperature (°C), diurnal temperature range (°C), total cloud fraction, soil moisture (volumetric water content fraction, depth of water per unit depth of soil), and sea level pressure (PSL, Pa) for southeast USA (SEUS), monthly means, *black* indicates base period 1961–1990, *red* is future 2080–2099, *horizontal lines* indicate mean frost day fraction, *vertical lines* are mean of values on horizontal axes, *diagonal lines* are best fit linear regression, and R^2 values and significance of linear regression coefficients are given in Table 2; *Right column*: same as left column except for northwest USA (*NWUS*)

ence) and future climate. However, as indicated in Fig. 4, the ensemble mean trend for relatively small decreases in frost days in Table 1 for the southeast US (–0.05 and –0.02 for reference and future, respectively) are not significant, while the decreases in the northwest USA are larger (–0.51 and –1.32) and significant. The decreasing trend in frost days in the present-day reference period for northern Europe are significant, but are not significant for future climate, while for eastern China the situation is the opposite with present-day decreases not significant, and future decreases significant. For both present and future climate, the decreasing trends in frost days for southeast Australia are significant. The trends for the anomalies, future minus present, reflect the results for the future trends.

To help better understand regional processes associated with the changes in frost days, we show ensemble mean trends in ensemble mean total annual frost days compared to cold season (ONDJFM for Northern Hemisphere, AMJJAS for Southern Hemisphere) frost days (reference period in Fig. 5a, future in Fig. 5b). Solid lines show annual values, dotted lines are cold season. As expected, there are somewhat fewer frost days for the cold season compared to the annual values since a few frost days occur outside the cold season. For most locations the differences are less than about 10 days, while the northwest USA has the biggest change from annual to cold season of about 30 days. This is due mainly to additional frost days occurring in September and April in addition to the cold season as defined here. In general the trend in annual frost days for the United States in Fig. 5a (and in Table 1) reflects the observations of Easterling (2002) shown in Fig. 1, with greater trends in decreasing frost days for the grid point chosen in the northwest USA (–0.51 days per year for present, –1.32 days per year in future) compared to the grid point in the southeast USA (no significant trend in either present or future). There are comparable numbers for cold season for the model (–0.43 days per year for present, –1.27 days per year for future). Trends in cold season frost days are reflected in the trends in annual values for the rest of the regions as well (not shown).

We now examine processes involved with cold season monthly values of frost days for present-day and future climate using two areas (southeast USA and northwest USA) to illustrate processes taking place in all regions. Previous studies have shown that changes in minimum temperatures, which we noted in Fig. 2, are related to changes in nighttime minimum temperatures and are usually related to changes in cloud fraction and soil moisture (Dai et al. 1999; Stone and Weaver, 2002). It was shown in Fig. 2 that nighttime minimum temperatures are related to frost days, so a starting point for processes relating to changes in frost days are factors that have been shown to affect minimum temperatures, and the related values of diurnal temperature range. Therefore, we plot cold season monthly values of frost days (fraction of frost days during the cold season) as a function of minimum temperature, diurnal temperature range, total cloud, soil moisture, and SLP for the two USA areas for present-day climate (in black in Fig. 6) and future climate (in red in Fig. 6). Both areas for present and future show a strong relationship between frost days and minimum temperature as could be expected from Fig. 2, with lower nighttime minimum temperatures associated with more frost days. The R^2 values (Table 2) for the regression of frost days on minimum temperature have values ranging from 0.82 to 0.87. The mean values of minimum temperature show an increase from present to future climate along with a corresponding decrease in the number of frost days in the top panels of Fig. 6.

Relationships with clouds, soil moisture, and diurnal temperature range show smaller R^2 values and some as low as 0 in Table 2. However there is a more consistent relationship with SLP in Table 2, with R^2 values generally larger compared to soil moisture and clouds (except for present climate for the northwest USA) in both regions. Thus on the monthly time scale, passing high pressure systems are associated with more frost days and lower nighttime minimum temperatures. Similar results occur for the other regions as indicated by the R^2 values and statistical significance (1% level) for the corresponding linear regression coefficients shown in Table 2. For all the areas for present and future climate, the SLP R^2 values are significant, but for diurnal temperature range, cloud, and soil moisture, the R^2 values are mostly

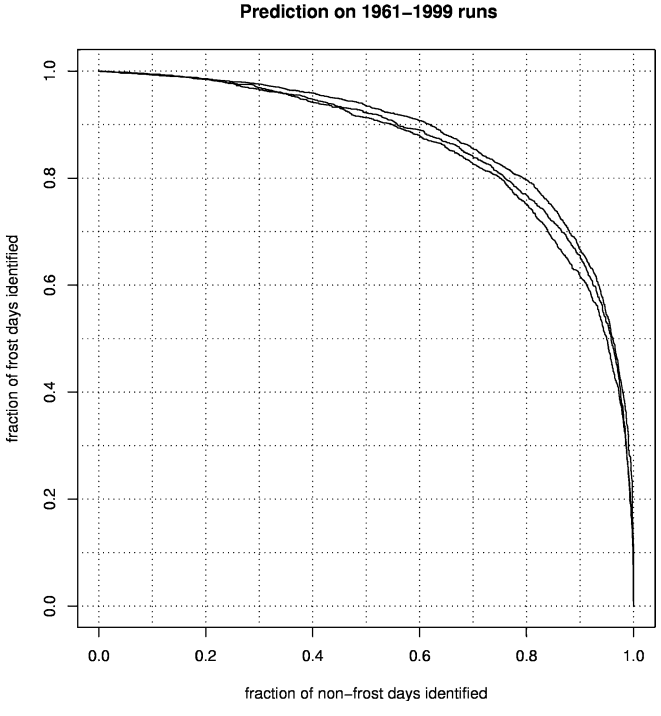

Fig. 7 Discrimination skills of statistical model for prediction of frost days. The panel shows a typical verification of model predictions on three ensemble members, after fitting the model's coefficients on the fourth ensemble member. All models, in both present and future periods and at all five locations, perform similar to the example here for southeast USA present. Further details are given in the Appendix 1

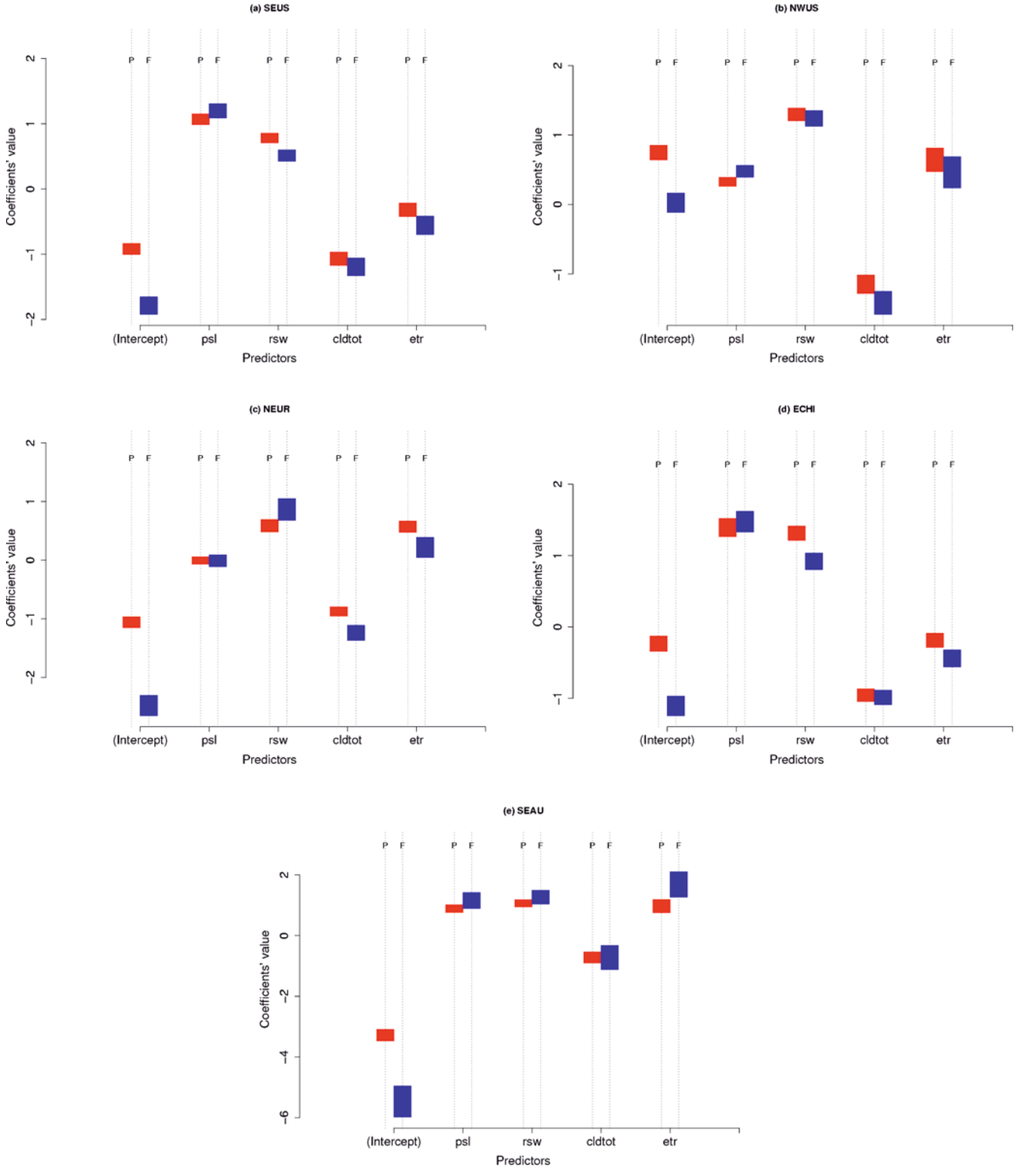

Fig. 8 **a** Results from multiple regression statistical model for southeast USA showing values of regression coefficients, *lengths* of *colored rectangle indicate* 95% confidence level, *P* indicates present-day climate (1961–1990), and *F* is for future climate (2080–2099), variables are from Eq. 1 as sea level pressure (*PSL*) soil moisture (*RSW*), total cloud (*CLDTOT*) and diurnal temperature range (*ETR*); **b** same as **a** except for northwest USA; **c** same as **a** except for Northern Europe; **d** same as **a** except for eastern China; **e** same as **a** except for southeast Australia

smaller and have a mixture of significance. For example, the two USA areas have significant contributions from soil moisture in present and future for the northwest USA where greater soil moisture produces enhanced latent heat flux, a cooler surface, lower nighttime minimum temperatures, and more frost days. But none of the other areas have significant contributions from soil moisture.

Meanwhile, Northern Europe and eastern China have significant contributions from cloud, but not soil moisture (not shown). In general, increased cloud reduces outgoing longwave radiation at night and contributes to higher nighttime minimum temperatures and fewer frost days. However, some areas, such as the northwest USA in present-day, show the opposite relationship mainly due to high clouds often occurring with high pressure, with the SLP relationship the stronger of the two to produce more frost days. Thus, for all areas the most consistently larger and significant R^2 values are from SLP.

Figure 6 shows two aspects of climate related to frost days. First, the scatter of the monthly values indicates the relationships on that time scale. Second, the mean values indicate the relationship to changes in the warmer base climate state in the future. Thus, average numbers of frost days are reduced in the two areas in Fig. 6, corresponding to mean values of diurnal temperature range that are lower (reflecting the greater increase of nighttime minima compared to daytime maxima), total cloud fraction that increases slightly, soil moisture has a very slight mean decrease in the southeast USA, while there are increases in the northwest USA, and for SLP there are increases in both regions (consistent with Fig. 3b). The higher mean SLP values in the future over the regions of interest noted in Fig. 3b are associated with fewer frost days and a tendency for somewhat greater cloud amount. Interestingly, on the monthly time scale, high pressure (episodically occurring in conjunction with passing high pressure systems and thus the absence of storminess) is associated with more frost days.

We also examined monthly mean changes of vertically averaged moisture (daily values were not saved from the model simulations), and we note a consistent relationship across all areas with positive moisture anomalies associated with fewer frost days. However, there is little consistent association of changes of moisture and frost days for the change in base state in the warmer future climate. Thus, the dominant processes are associated with the high pressure anomalies that produce fewer frost days in the future climate due to regional scale changes of atmospheric circulation (discussed earlier) that advect warmer air into the regions of interest and contribute to elevated nighttime minimum temperatures.

5 Statistical model of frost day changes

Next, we formulate and estimate, separately for each of the five areas, a statistical model that aims at quantifying the combination of processes involved in the changes in occurrence of frost days. We adopt the framework of a logistic regression, a member of the family of generalized linear models (McCullagh and Nelder 1998)

Logistic regression is a generalization of linear regression to the case where the outcome is a probability lying between 0 and 1. In our case, we are interested in modeling the probability of occurrence of a frost day, p_f (probability of the minimum temperature falling below 0 °C) as a function (linear after transformation) of sea level pressure (PSL) soil moisture (RSW), total cloud (CLDTOT) and diurnal temperature range (ETR). We do so by estimating the coefficients of the regression:

$$\log\ p_f/1 - p_f = a + (b_1 \times\ \mathrm{PSL}*) + (b_2 \times\ \mathrm{RSW}*\ ) + (b_3\ \times\ \mathrm{CLDTOT}*) + (b_4 \times\ \mathrm{ETR}*) \quad (1)$$

where the asterisks indicate that the variables have been standardized with respect to the reference period's ensemble means and standard deviations.

Once the coefficients a, $b1$, $b2$, $b3$, and $b4$ are estimated, the statistical model predicts, for any given day in the ensemble runs, a probability of occurrence of a frost day, p_f', as a function of that day's values of PSL, RSW, CLDTOT and ETR. Predictions can be performed by choosing a threshold (usually but not necessarily 0.5) and labeling the day as a frost day if the predicted p_f' is above that threshold. Protection against false positives is achieved by setting the threshold relatively high, at the risk of identifying only a small fraction of frost days. Conversely, as a protection against false negatives, a lower threshold would guarantee the identification of a larger fraction of frost days, but would likely mislabel, as frost days, many days in which the minimum temperature stayed above 0 °C. Thus, the performance of the model in predicting frost days has to balance a trade-off between the fraction of frost days incorrectly identified (false negatives) and the fraction of non-frost days incorrectly identified (false positives).

A perfect model (i.e., a model estimating an exact relation between PSL, RSW, CLDTOT and ETR, and the occurrence of a frost day) would identify, for an appropriate choice of the threshold on p_f', 100% of frost days, and 100% of non-frost days. A model without skill could do no better than a toss of a coin, identifying only 50% of both.

The coefficients a, $b1$, $b2$, $b3$, and $b4$ in Eq. 1 are estimated by fitting the regression to the data derived from one of the ensemble members. Predictions for the

Fig. 9 **a** Growing season length (GSL) for southeast USA for 1961–1990 (*blue*) and 2080–2099 (*red*), **b** *solid straight lines* are ensemble means, *solid lines* are range of ensemble members; **c** and **d** same as **a** and **b**, respectively, except for northwest USA; **e** and **f** same as **a** and **b**, respectively, except for Northern Europe; **g** and **h** same as **a** and **b**, respectively, except for eastern China; **i** and **j** same as **a** and **b**, respectively, except for southeast Australia

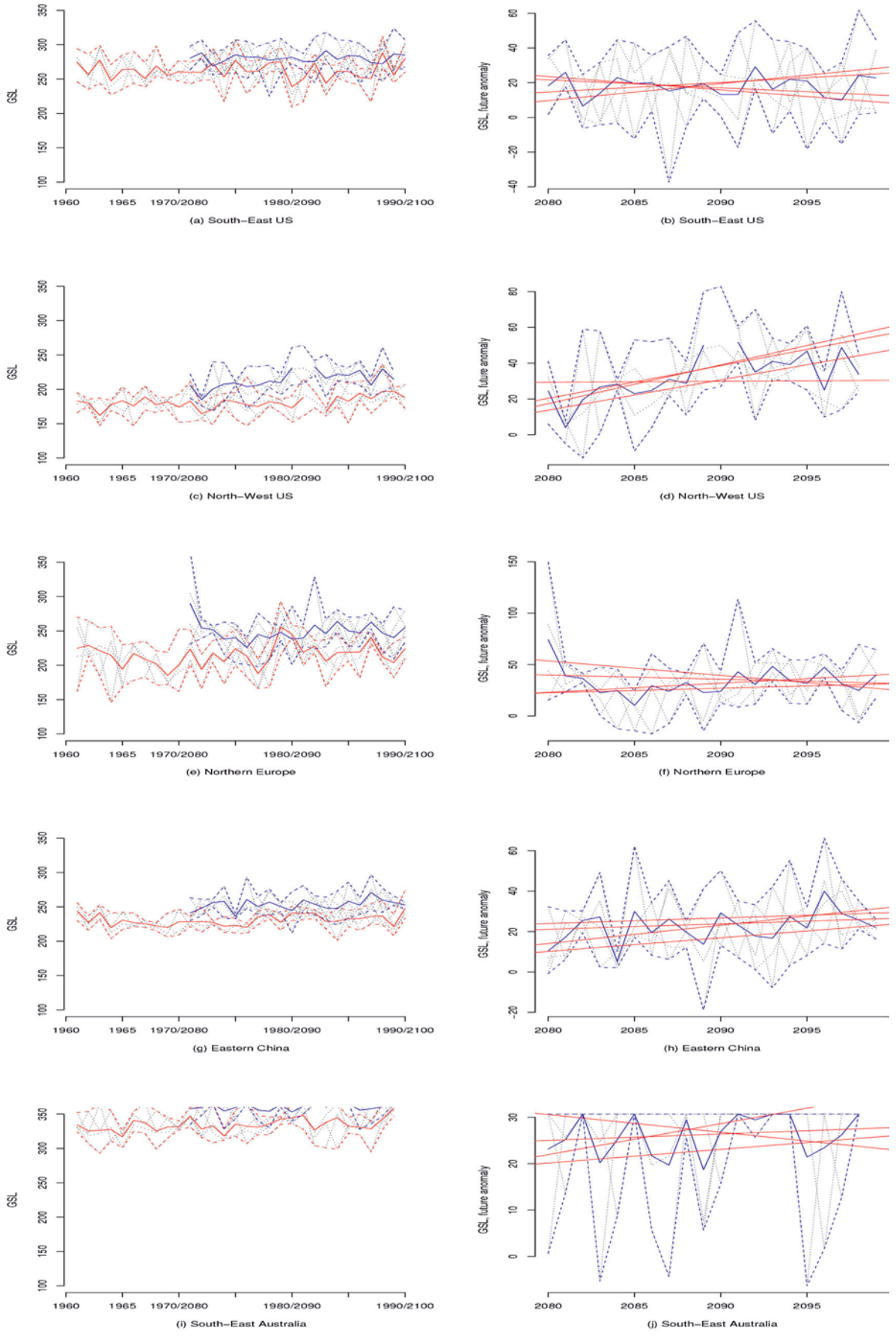
GSL
GSL, future anomaly
1960
1965
1970/2080
1980/2090
1990/2100
2080
2085
2090
2095
(a) South–East US
(b) South–East US
(c) North–West US
(d) North–West US
(e) Northern Europe
(f) Northern Europe
(g) Eastern China
(h) Eastern China
(i) South–East Australia
(j) South–East Australia

remaining three ensemble members are obtained each day by applying the estimated coefficients to the values of PSL, RSW, CLDTOT and ETR in their respective time series.

Figure 7 shows the performance of one of the regression models, estimated for one of the 5 locations. The models for the remaining four locations (not shown) look very much the same. We describe in the Appendix the computations required to draw the curve, and its exact significance. This curve is just a variant of the ROC curves that are a well established means of verification for statistical models of the kind of Eq. 1. The important message to be derived from Fig. 7 is the existence of an adequate threshold for p_f', by whose choice we can predict as accurately as 80% of frost days, and 75 to 80% of non-frost days at the same time (the three curves shown passing through or above a point in Fig. 7 with such coordinates) for all three of the independently predicted ensemble members, that is, by estimating the regression on one of the four, and verifying the accuracy of the prediction on the other three. All the five regions' regressions behave almost identically (not shown), thus proving the robustness of the statistical model (Eq. 1).

Similarly, recalculating the coefficients for future climate and using the same technique allows the fitting of the relationships among processes in one of the ensemble members to accurately predict the remaining three, for all five areas. This is despite a shift in the average number of frost days from the present to the future climate that characterizes all of the five regions' statistics. Having estimated the functional form of Eq. 1 for present and future simulations allows us to examine the details of this shift as it is measured by the statistical model.

Figure 8 shows, for each region separately, a comparison between the values of the coefficients in Eq. 1 estimated for the present (blue rectangles in the figure, marked by a "*P*" above), with respect to those estimated for the future climate (red rectangles, marked by an "*F*" above). The height of the rectangles indicates the 95% confidence interval for each of the coefficients. Note that for each region, and for each of the predictors, there is at most a very slight disagreement between the ranges for present and future climates. That is, there is overlap between the blue and red rectangles. However, the intercept is significantly different (no overlap) for all five areas. This suggests that the physical relationships among the processes that contribute to changes in frost days are the same for all areas for present and future climates, but the change in average climate base state is indicated by the significant change in the intercept. Therefore, physical interactions that produce decreases in frost days do not change in future climate. The only significant change is in the average base state.

6 Relationship to growing season length

One implication for decreases in frost days is a longer growing season. To examine this possibility, we use the definition given by Frich et al. (2002). Growing season length is defined as the number of days between the first occurrence of at least six consecutive days with mean temperature greater than 5 °C, and the first occurrence, after July 1st (January 1st in the Southern Hemisphere), of at least six consecutive days with mean temperature less than 5 °C. Figure 9 shows that, for each of the five regions, growing season length increases (in association with the decrease in frost days shown in Fig. 2a). However, the relationship between decrease in frost days and increase in growing season length is not as significant as, say the correlation between frost days and minimum temperatures shown in Fig. 6 and Table 2. Figure 10 shows plots of annual frost days plotted against growing season length. The R^2 values range from 0.0 to 0.57, indicating other factors, in addition to frost days, contribute to growing season length in the various regions. Exploring these more complicated relationships is beyond the scope of the present work, and will be the subject of a future study.

Fig. 10 **a** Growing season length plotted as a function of frost days (yearly values), solid line is linear correlation; southeast USA 1961–1990; **b** same as **a** except for 2080–2099; **c** and **d** same as **a** and **b**, respectively, except for northwest USA; **e** and **f** same as **a** and **b**, respectively, except for northern Europe; **g** and **h** same as **a** and **b**, respectively, except for eastern China; **i** and **j** same as **a** and **b**, respectively, except for southeast Australia

7 Conclusions

A global coupled climate model is run for ensemble simulations of twentieth century climate, and changes in twentyfirst climate in a business as usual scenario (nearly the average of the SRES scenarios) and these simulations are examined in relation to frost days (days with nighttime minimum temperatures below 0 °C). A comparison of trends in frost days for the second half of the twentieth century over the USA from observations and the model shows the model is capable of simulating the general annual pattern of greater decreases in frost days over the western and southwestern USA, with almost no changes of frost days over the upper Great Plains, upper Midwest and northeastern USA. Additionally, both observations and model show almost no changes of frost days for the fall season, but a comparable pattern, with decreased amplitude, of frost day changes for spring compared to the annual values.

By the end of the twentyfirst century in the model, frost days decrease everywhere, but the pattern of the changes is shown to depend partly on regional changes in circulation. Thus air is advected from different directions such that frost days decrease most over the western parts of the continents, with a southwest to northeast gradient of frost day decreases, and fewer frost day decreases to the northeast. This pattern of frost day decreases is related to increases in nighttime minimum temperatures in the future climate, but these increase

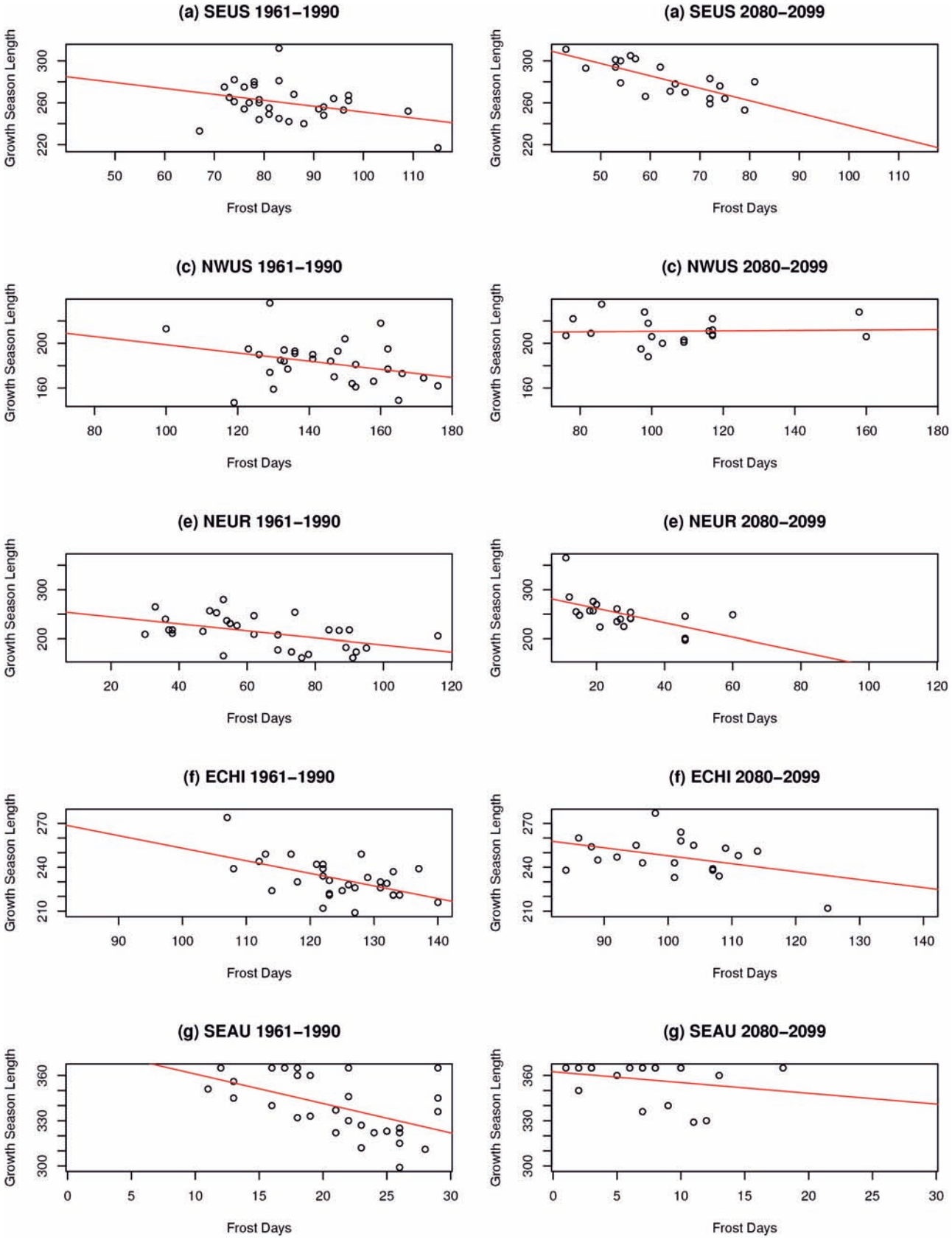
(a) SEUS 1961–1990
(a) SEUS 2080–2099
(c) NWUS 1961–1990
(c) NWUS 2080–2099
(e) NEUR 1961–1990
(e) NEUR 2080–2099
(f) ECHI 1961–1990
(f) ECHI 2080–2099
(g) SEAU 1961–1990
(g) SEAU 2080–2099
Growth Season Length
Frost Days

steadily poleward, while frost day decreases are diminished farther poleward. This is due to the fact that frost days decrease most in marginal areas near 0 °C. Areas farther poleward have nighttime minima that remain below 0 °C for the most part and thus experience fewer changes of frost days.

Five regions are chosen to examine processes that contribute to the changes in frost days. Factors associated with changes in cloud and soil moisture have been identified earlier as playing roles in increases in nighttime minimum temperatures in future warmer climates as well as with decreasing diurnal temperature range. However, these do not contribute as consistently as do changes in sea level pressure to the regional decrease in frost days. This is interpreted as an indication of regional changes in atmospheric circulation that play the most consistent role in decreasing frost days, with changes in cloud, soil moisture and diurnal temperature range making contributions for some time periods in some regions, but generally playing secondary roles.

A multiple regression statistical model is employed to quantify the relationships among the processes contributing to decreases in frost days. It is demonstrated that the coefficients for the processes associated with frost days (soil moisture, clouds, diurnal temperature range, and sea level pressure) have comparable interactions and contributions in present and future climates. The largest change is in the intercept, indicating that physical processes are not changed in their interactions between present and future climates, but the changes in the average base state climate (i.e., temperature) are the most marked and significant.

Though growing season length decreases at all five areas where frost days also decreased, correlations between annual frost days and growing season length are not high, indicating other factors in addition to frost days also determine changes in growing season length.

Acknowledgements The authors acknowledge the contribution of Robert Tomas for compiling the ENSO statistics from the model. This work was supported in part by the Weather and Climate Impact Assessment Initiative at the National Center for Atmospheric Research. A portion of this study was also supported by the Office of Biological and Environmental Research, USA Department of Energy, as part of its Climate Change Prediction Program, and the National Center for Atmospheric Research. The National Center for Atmospheric Research is sponsored by the National Science Foundation.

Appendix 1

Curves like those shown in Fig. 7 are sometimes defined "probability of detection" (POD) curves, and are an effective way of verifying the performance of a statistical prediction when the outcome is a binary variable, 0 or 1 or, in our case, non-frost day or frost day.

The statistical model in Eq. 1 produces a prediction of the probability p_f of the minimum temperature falling below 0 °C for each day used for verification. An actual prediction of frost-day demands the arbitrary choice of a threshold, a value t between 0 and 1 such that for any day's predicted value p_f', the day will be predicted as a frost-day if $p_f' \geq t$, otherwise it is a non-frost day.

For any given choice of a threshold, values of (a) the fraction of correctly identified frost days (sometimes called "probability of detection of 1's, or POD 1") and (b) the fraction of correctly identified non-frost days (sometimes called "probability of detection of 0's or POD 0") can be easily computed by building a two-way table of predicted versus true frost days:

	T0	T1
P0	n00	n01
P1	n10	n11

In the two way table, n00 is the number of days correctly predicted as non-frost days, $n01$ is the number of frost days incorrectly predicted as non-frost days, $n10$ is the number of non-frost days incorrectly predicted as frost days and $n11$ is the number of frost days correctly predicted. The fraction in (a) is given by $n11/(n11+n01)$; the fraction in (b) is given by $n00/(n00+n10)$.

For any real-life prediction (i.e., for any non-perfect model), the two PODs are constrained by a trade-off. The higher t (the higher we demand p_f' to be before labeling a day "frost-day"), the lower will be the number of days in the P1 row, so the lower POD 1 and the higher POD 0 (protecting against false positives). Conversely, the lower t, the higher will be the number of days in the P1 row, so the higher POD1 and the lower POD0.

The better the model, the higher the values of POD0 and POD1 will be at the same time. A perfect model would be able to achieve 100% in both PODs at the same time ($n10 = n01 = 0$). A bad model could do no better than chance, identifying only 50% of both. All intermediate models will achieve pairs of values for POD0 and POD1 between 0.5 and 1, differently balancing the two as a function of the threshold t chosen.

Any given model's prediction can be represented by a POD curve, with each point on the curve having coordinates given by the values of POD0 and POD1 corresponding to a value of the threshold t. The better the model, the higher towards the upper right corner the POD curve will be. Perfect predictions would be represented by a curve overlaying the upper and right sides of the plotting region, reaching 100% in both coordinates.

No-skill predictions would be represented by straight lines joining the upper left to the lower right corners (through the 50%–50% point).

References

Ammann C, Meehl GA, Washington WM, Zender C (2003) A monthly and latitudinally varying volcanic forcing data set in simulations of twentieth century climate. Geophys Res Lett 30: 10.1029/2003GLO16875RR

Bonsal BR, Zhang X, Vincent LA, Hogg WD (2001) Characteristics of daily and extreme temperatures over Canada. J Clim 14: 1959–1976

Cubasch U, Meehl Ga, Boer GJ, Stouffer RJ, Dix M, Noda A, Senoir CA, Raper S, Yap KS (2001) Projections of future climate change. In: Houghton JT, Ding Y, Griggs DJ, Noguer P, van der Linden P, Dai X, Maskell K, Johnson CI (eds) Climate change 2001: The Scientific Basis. Contribution of Working Group I to the Third Assessment Report of the Intergovernmental Panel on Climate Change. Cambridge University Press, Cambridge UK, pp 525–582

Dai A, Trenberth KE, Karl TR (1999) Effects of clouds, soil moisture, precipitation, and water vapor on diurnal temperature range. J Clim 12: 2451–2473

Dai A, Wigley TML, Boville BA, Kiehl JT, Buja LE (2001) Climates of the twentieth and twenty-first centuries simulated by the NCAR Climate System Model. J Clim 14: 485–519

Delworth TL, Mahlman JD, Knutson TR (1999) Changes in heat index associated with CO2-induced global warming. Clim Change 43: 369–386

Easterling DR, Meehl GA, Parmesan C, Changnon S, Karl TR, Mearns LO (2000) Climate extremes: observations, modeling and impacts. Sci 289: 2068–2074

Easterling DR (2002) Recent changes in frost days and the frost-free season in the United States. Bull Am Meteorol Soc 83: 1327–1332

Frich P, Alexander LV, Della-Marta P, Gleason B, Haylock M, Klein Tank AMG, Peterson T (2002) Observed coherent changes in climate extremes during the second half of the twentieth century. Clim Res 19: 193–212

Fyfe JC, Boer GJ, Flato GM (1999) The Arctic and Antarctic Oscillations and their projected changes under global warming. Geophys Res Lett 26: 1601–1604

Gillett NP, Allen MR, McDonald RE, Senior CA, Shindell DT, Schmidt GA (2002) How linear is the Arctic Oscillation response to greenhouse gases? J Geophys Res 107: 10.1029/2001JD000589

Heino R and coauthors (1999) Progress in the study of climate extremes in northern and central Europe. Clim Change 42: 151–181

McCullagh P, Nelder JA (1998) Generalized linear models, 2nd edn. Chapman and Hall/CRC, London

Meehl GA, Zwiers F, Evans J, Knutson T, Mearns L, Whetton P (2000) Trends in extreme weather and climate events: issues related to modeling extremes in rojections of future climate change. Bull Am Meteorol Soc 81: 427–436

Meehl GA, Gent P, Arblaster JM, Otto-Bliesner B, Brady E, Craig A (2001) Factors that affect amplitude of El Nino in global coupled climate models. Clim Dyn 17: 515–526

Meehl GA, Washington WM, Wigley TML, Arblaster JM Dai A (2003) Solar and greenhouse forcing and climate response in the 2othe century. J Clim 16: 426–444

Meehl GA, Washington WM, Arblaster JM, Hu A (2004a) Factors affecting climate sensitivity in global coupled models. J Clim 17: 1584–1596

Meehl, GA, Washington WM, Ammann C, Arblaster JM, Wigley TML, Tebaldi C (2004b) Combinations of natural and anthropogenic forcings and 20th century Climate. J Clim in press

Parmesan C, Root TL, Willig MR (2000) Impacts of extreme weather and climate on terrestrial biota. Bull Am Meteorol Soc 81: 443–450

Stone DA, Weaver AJ (2002) Daily maximum and minimum temperature trends in a climate model. Geophys Res Lett 29: 10.1029/2001GL14556

Washington WM, Weatherly JW, Meehl GA, Semtner Jr. AJ, Bettge TW, Craig AP, Strand Jr. WG, Arblaster JM, Wayland VB, James R, Zhang Y (2000) Parallel climate model (PCM) control and transient simulations. Clim Dyn 16: 755–774